Case Studies in Construction Materials 17 (2022) e01160

Contents lists available at ScienceDirect

Case Studies in Construction Materials

journal homepage: www.elsevier.com/locate/cscm

Case study

Shear performance of lightweight concrete filled hollow flange cold-formed steel beams

Mohamed Sifan [a,*], Perampalam Gatheeshgar [a,b], Brabha Nagaratnam [a], Keerthan Poologanathan [a], Satheeskumar Navaratnam [c], Julian Thamboo [d], Marco Corradi [a,e]

[a] Department of Mechanical and Construction Engineering, Northumbria University, Newcastle upon Tyne, UK
[b] School of Computing, Engineering and Digital Technologies, Teesside University, Middlesbrough, UK
[c] School of Engineering, RMIT University, Melbourne, Australia
[d] Department of Civil Engineering, South Eastern University of Sri Lanka, Oluvil, Sri Lanka
[e] Department of Engineering, University of Perugia, Italy

ARTICLE INFO

Keywords:
Hollow flange cold-formed steel beam
Concrete infill
Lightweight concrete
Composite beams
Ultimate shear capacity
Numerical analysis
Design guidelines

ABSTRACT

Concrete-infilled hollow flange cold-formed steel (CF-HFCFS) beams have gained attention in the construction practices owing to many benefits in terms of their structural performances and applicability. The concrete infill ensures better structural performance by restraining the buckling instabilities of thin-walled cold-formed steel elements. However, the shear strength characteristics of CF-HFCFS are not systematically explored yet and hence there is a lack of understanding on the shear strength characteristics of CF-HFCFS beams. Therefore, in this research, shear characteristics were investigated through numerical studies by establishing and analysing three-dimensional finite element (FE) models of CF-HFCFS beams. The developed FE models were verified against the experimental data in terms of failure modes, ultimate shear capacities, and load-displacement characteristics. Then a series of parametric analyses were carried out to investigate the shear behaviour of CF-HFCFS beams against the effects of geometrical (steel thickness, beam depth) and mechanical (yield strength of steel and compressive strength of concrete) properties to further verify the shear characteristics of CF-HFCFS. Lightweight normal and lightweight high strength concrete materials were considered as infill. Also, the influence of the concrete infill on the ultimate shear capacity of the CF-HFCFS beams was evaluated through parametric studies. The ultimate shear capacities were compared against the already available design provisions. Consequently, based on the data established through of parametric analyses, modified design provisions are developed to estimate the ultimate shear capacity of CF-HFCFS beams.

* Corresponding author.
E-mail addresses: sifan.i.sifan.mohamed@northumbria.ac.uk (M. Sifan), g.perampalam@tees.ac.uk (P. Gatheeshgar), brabha.nagaratnam@northumbria.ac.uk (B. Nagaratnam), keerthan.poologanathan@northumbria.ac.uk (K. Poologanathan), sathees.nava@rmit.edu.au (S. Navaratnam), jathamboo@seu.ac.lk (J. Thamboo), marco.corradi@northumbria.ac.uk (M. Corradi).

https://doi.org/10.1016/j.cscm.2022.e01160
Received 24 February 2022; Received in revised form 27 April 2022; Accepted 12 May 2022
Available online 16 May 2022

1. Introduction

The cold-formed steel (CFS) beams have become more popular in the building sector, especially in lightweight construction systems, due to its outstanding structural and cost-effective properties [1,2]. Hollow flange cold-formed steel (HFCFS) beams have been increasingly used as they have shown capabilities of resisting local buckling, distortional buckling, and lateral-torsional buckling (LTB) compared to the other conventional CFS beams. Numerous studies have been reported in terms of improving its flexural, shear, web crippling, resistances and enhancing the overall structural performance by evaluating the effect of stiffened edges and web holes in HFCFS beams [3–5]. Subsequently, rational design provisions have been developed through various research studies to characterise the flexural and shear characteristics of HFCFS beams [2,5]. However, still the HFCFS beams are prone to local buckling in the compression flanges and needed more investigation to minimize the phenomenon.

Then an idea of infilling concrete inside the hollow flanges of HFCFS beams was introduced to prevent or delay the local buckling of flanges, because they undergo compression and are prone to local buckling. Subsequently, concrete filled hollow flange cold-formed steel (CF-HFCFS) beams have been popularised by the various application in buildings and bridges as these beams provide high load carrying capacity, stability, high speed in construction, high energy absorption and higher stiffness compared to other conventional HFCFS [6–9]. There have been few studies conducted to evaluate the flexural, shear, LTB, and local buckling resistance of CF-HFCFS beams using experimental, analytical, and numerical methods [2,6–8,10–12]. All of these studies concluded that the concrete infill significantly improve the overall structural performance in terms of their resistance and stiffness. However, the self-weight of the concrete might negatively affect the stability of the member and the construction process.

Therefore, replacing the normal weight concrete (NWC) with lightweight concrete (LWC) as the filling material in CF-HFCFS beams could create a cost-effective solution, given the reduced production and transportation costs [13–15]. Furthermore, LWC has significant benefits such as reduced self-weight, better sound resistance and thermal insulation, higher fire resistance, acoustic absorption, and frost resistance. However, very limited studies have been conducted on LWC filled CFS beams. Al-Shaar and Gǒğüş [15] experimentally studied the flexural performance of LWC filled steel tube section and stated that these composite beams had the potential to replace normal weight CFS beams. Abou-Rayan et al. [16] investigated the effect of LWC infill on the flexural performance of HFCFS beams and stated that the presence of LWC can increase the flexural capacity by 40%.

Because of the advantages of LWC, researchers are working to reduce the density of high strength concretes, resulting in high strength LWC, which might be a superior alternative for normal weight high strength concrete in terms of sustainability [17–19]. Numerous research studies have facilitated the development of high strength LWC by using only fine aggregate (aggregate nominal size less than 4.75 mm) [20] with lightweight aggregate to make the concrete more flowable, homogeneous, and strong [21–23]. An example of such concrete type, is ultra-lightweight cementitious composite (ULCC), which is often constructed from cenosphere (particle size less than 300 μm), a waste material from coal power plants [19,24–27]. The compressive strength of ULCC is usually greater than 60 MPa with densities around 1500 kg/m^3, which is around 42% less than NWC. Thus, these types of high strength LWC are more suitable for filling inside very small steel tubes such as the hollow flanges of even small CFS beam sections without inducing instability to the section.

Therefore, incorporating these types of lightweight high strength concrete filled HFCFS beams would be beneficial for the construction industry, especially in modular building construction as it requires structural members with reduced self-weight. Moreover, the influence of the infilled concrete on the instability of the web is comparatively low for LWC compared to NWC. This is because HFCFS beams are vulnerable to undergoing geometric imperfection, if the weight of infill is high as the web thickness of the beams is relatively low compared to hot rolled sections [28]. Consequently, Sifan et al. [28] recently investigated the flexural performance of HFCFS beams filled with normal and high strength lightweight concrete and revealed that the concrete infill can contribute up to 55% flexural capacity increment in CF-HFCFS beams than that of bare HFCFS beams.

The shear performance of CF-HFCFS beams filled with LWC is one of the crucial parameters to be verified in the design. This is because the shear failure is often the predominant failure mechanism in CF-HFCFS beams, if the effective span is short. There are few studies that investigated the shear behaviour of steel beams with concrete-filled hollow flange sections. Hassanein [6] numerically studied the shear performance of concrete-filled pentagonal flange steel beams by applying point load at the mid-span and stated that shear load capacity was increased due to the presence of concrete, which contributed to the stiffness of the upper flanges. Furthermore, the shear strength was increased by decreasing the aspect ratio of the web. Wang et al. [29] conducted experimental tests to investigate the flexural and shear behaviour of concrete-filled tubular flanged I-girders with short span and with corrugated web, and concluded that the corrugated web improved the ultimate load carrying capacity by 43%. Further, based on numerical and theoretical analyses Wang et al. [30] proposed, a simplified equation to predict the shear capacity. However, to authors' best of knowledge, there are no studies related to the pure shear behaviour of doubly symmetric HFCFS beams filled with lightweight concrete and no systematic design guideline in predicting the shear strength characteristics is available in the literature.

Hence, this study focuses on FE numerical investigation of the shear performance of doubly symmetric HFCFS beams filled with normal and high strength lightweight concrete. Consequently, 3D FE numerical models were developed for both with and without concrete filled HFCFS beams. The developed models were validated against the available experimental results to ensure the accuracy of the prediction. The validated models were then extended to conduct a parametric study to examine and compare the effect of lightweight concrete infill, and the influential parameters including the geometrical and steel strength characteristics. The simulation data were then used to develop a design guideline by using the Direct Strength Method (DSM) with reasonable accuracy to predict the ultimate shear capacity of LWC filled HFCFS beams.

2. FE numerical simulation

2.1. General

A commercially available finite element (FE) based package, ABAQUS (2021) [31] was used to develop and extensively analysis the behaviour of CF-HFCFS beams under shear actions. The composite CF-HFCFS beam consisted of three major parts, which were the HFCFS beam, concrete infill, and web support plates (WSPs). In this study, both CF-HFCFS and bare HFCFS beam FE models were developed to study the effect of infilled lightweight concrete on the shear capacities of CF-HFCFS beams. Most of the modelling techniques used in this study were successfully employed by the authors' previous studies [5,28,32,33]. The failure modes, force-displacement relationships and ultimate loads obtained from the FE model analysis were compared with previous experimental studies to validate the modelling techniques against shear action.

2.2. FE model development

The accuracy and efficiency of the FE model predictions are depending on the suitable mesh density, element type and the material properties. Shell elements (S4R) with four-node reduced integration were incorporated to model the HFCFS beam, whereas concrete was represented using eight-node brick elements (C3D8R) as shown in Fig. 1. These elements were more suitable to predict the structural behaviour of both cold-formed steel and concrete of concrete-steel composite structures [30,34]. The WSPs were modelled with four-node rigid quadrilateral (R3D4) elements. In order to identify the appropriate mesh size, this study employed the convergence study, and the results show that a mesh size of 5 × 5 mm was appropriate to model both HFCFS beam and concrete. Moreover, the WSPs were meshed with 10 × 10 mm elements [32]. A typical model contains more than 14544 and 6969 S4R and C3D8R elements, respectively.

Two different material models were considered for cold-formed steel and lightweight concrete. Yun and Gardner [35] and Afshan et al. [36] highlighted that the stress-strain relationship of cold-formed steel shows a gradually yielding response trailed by a substantial period of strain hardening. Thus, the elastic-perfectly plastic model with nominal yield strength can be used to predict the structural response of elements made with cold-formed steel [37–39]. The Young's modulus of 200 GPa and Poisson's ratio of 0.3 were used for the cold-formed steel in the analyses. The concrete material was modelled with Concrete Damage Plasticity (CDP) material model available in ABAQUS [31], since concrete mainly fails by crushing with compression and cracking with tension. Subsequently, the behaviour of lightweight concrete is different from normal weight concrete, the properties of lightweight concrete need to be carefully chosen for accurate prediction. The Poisson's ratio was chosen as 0.2, and the Eqs. (1–3) were adopted from detailed research conducted by Lim and Ozbakkaloglu [40] to calculate the Young's modulus (E_c) and to plot the compressive stress-strain relationship of the confined lightweight concrete.

$$E_c = 4400\sqrt{f'_{co}}\left(\frac{\rho_{c,f}}{2400}\right)^{1.4} \tag{1}$$

$$f_c = \frac{f^*_{cc}\ (\varepsilon_c/\varepsilon^*_{cc})r}{r-1+(\varepsilon_c/\varepsilon^*_{cc})^r} \quad if \quad 0 \le \varepsilon_c \le \varepsilon^*_{cc} \tag{2}$$

$$f_c = f^*_{cc} - \frac{f^*_{cc} - f_{c,res}}{1+\left(\frac{\varepsilon_c - \varepsilon^*_{cc}}{\varepsilon_{c,i} - \varepsilon^*_{cc}}\right)^{-2}} \quad if \quad \varepsilon_c \ge \varepsilon^*_{cc} \tag{3}$$

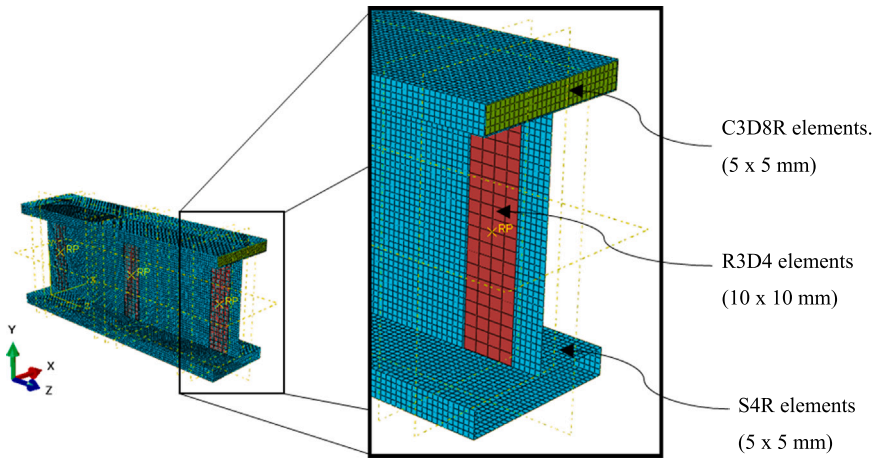

Fig. 1. Mesh refinement of CF -HFCFS beam model.

Where, f'_{co} is compressive strength, $\rho_{c,f}$ is density of lightweight concrete. f_c and f^*_{cc} are confined and unconfined compressive stress, respectively. Also, ε_c and ε^*_{cc} are the corresponding confined and unconfined stain. $f_{c,res}$ is the residual stress and $\varepsilon_{c,i}$ is inflation point at the post peak curve.

Eqs. (4) and (5) represent the tensile stress-strain behaviour of lightweight concrete. Al Zand et al. [39] satisfactorily applied the Eq. (5) to simulate the tensile post-peak behaviour.

$$f_t = E_c \quad \varepsilon_t \quad if \quad \varepsilon_t \leq \varepsilon_{lctm} \tag{4}$$

$$f_t = f_{lctm} \quad (\varepsilon_{lctm}/\varepsilon_t)^{0.8} \quad if \quad \varepsilon_t > \varepsilon_{lctm} \tag{5}$$

Where, f_t is tensile stress, ε_t is tensile strain, f_{lctm} and ε_{lctm} are tensile strength and corresponding tensile strain, respectively. All of these expressions were successfully employed by Sifan et al. [28] to simulate the behaviour of lightweight concrete inside doubly symmetric HFCFS beams under flexural action.

The surface-to-surface interaction function in ABAQUS [31] was used to provide penalty friction contact between steel and concrete interaction surfaces. The friction coefficient of 0.57 was used to simulate the tangential behaviour of interaction between steel and concrete [28]. Whilst "Hard contact" was employed to simulate the normal behaviour of the contact. A similar methodology was employed by the past research [41,42] and results show that the method can capture the realistic interaction behaviour the cold-formed steel to concrete.

Both HFCFS and CF-HFCFS beams were modelled in full length with a three-point loading arrangement as shown in Fig. 2. In each model, three WSPs were attached by using the "tie" constraint individually at the supports and the loading line to prevent any bearing failure at these locations. To generate the three-point loading, boundary conditions were assigned at the reference points (RP) of the rigid WSPs. While translational DOFs (degree of freedom) in "x", "y", and "z" directions were restrained at the pin, only "x" and "y" were restrained at the roller support to simulate the simply supported boundary condition. A displacement-controlled loading was applied at the middle WSP. In both the supports and the loading point as well as outer surfaces of the flange near the support and loading line, the rotational DOF in the "z" direction was restrained to prevent the lateral torsional buckling (LTB) and to generate pure shear failure.

The geometric imperfection was taken into account as it affects the shear capacity of the HFCFS beams with small thicknesses. Initially, a linear elastic buckling analysis was conducted and the critical buckling mode was selected to scale and import into the perfect geometry with the magnitude of $d_1/150$ [43,44]. Where, d_1 is the clear height of the web. Since the buckling has occurred on the web, the buckling effect of the flanges was ignored as it was found to be less influential as per the previous studies [30,45]. The different buckling modes obtained and the corresponding buckling loads are presented in Fig. 3.

2.3. Validation of FE numerical models

The developed numerical Finite Element (FE) models were then validated with available experimental results reported in the literature [5,29]. It should be noted that there are no comprehensive experimental results for doubly symmetric hollow flange CFS beams that failed predominantly in shear. The assumed modelling techniques were validated against the existing shear test results for CFS Litesteel beams (mono-symmetric hollow flange) reported in previous studies [5,46]. Therefore, the ability of the assumed modelling techniques against predicting the ultimate shear strength, load-displacement response, and failure modes of HFCFS sections without infill can be assessed. The geometric imperfection of $d_1/150$ was employed in the FE model, while measured geometric and

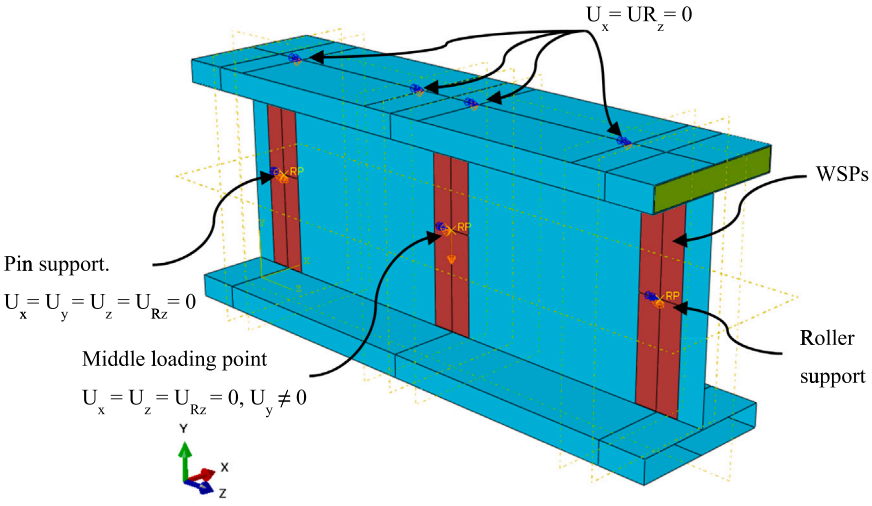

Fig. 2. Assigned boundary conditions of CF-HFCFS beam model.

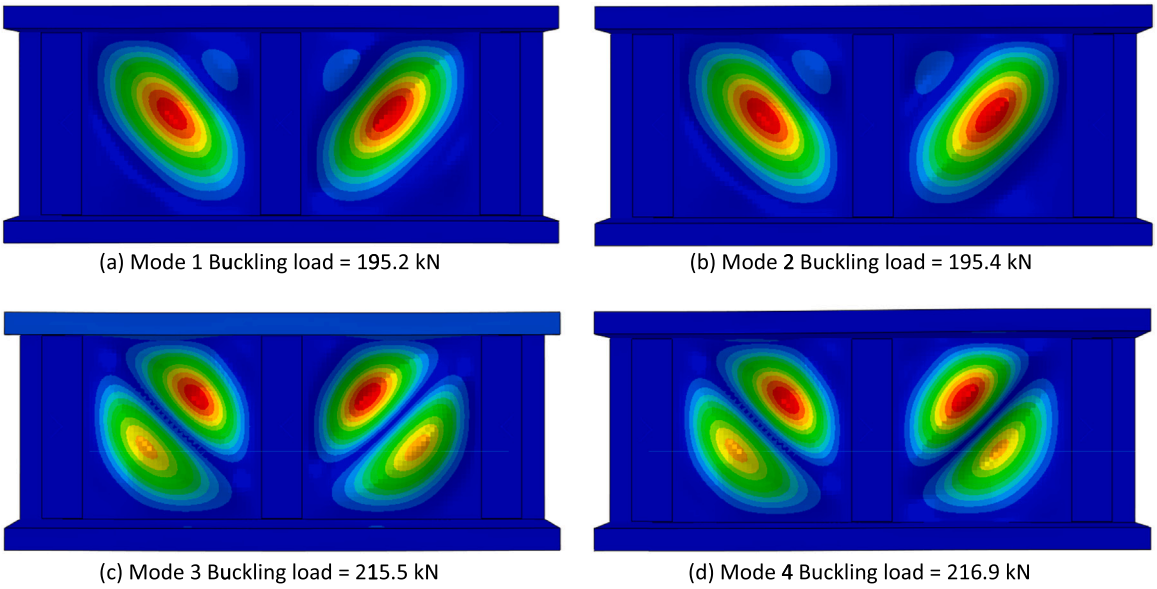

Fig. 3. Buckling modes and the buckling loads.

material properties were considered to generate the model.

Additionally, the ability of the generated FE models to predict the shear behaviour of concrete filled doubly symmetric hollow flange sections was validated against an experimental results provided in Wang et al. [29], where a I-girder (specimen name FWG) with a short span of beam were tested with three point loading to investigate the flexural and shear yielding. To mimic the models, the dimensions, boundary conditions and the material properties were carefully substituted. The beam dimensions are shown in the Fig. 4. The compressive strength of the infilled concrete was 31.2 MPa. The model and the test were compared in terms of ultimate load, failure mechanism, and load-displacement relationship.

Altogether, seven shear test results were selected for the validation. Table 1 summarises the comparison of the ultimate shear loads predicted by the FE models with the shear test results. The statistical evaluations, the mean and Coefficient of Variation (COV) indicated a high degree of accuracy in predicting ultimate shear strength, where the mean value is 0.99 and the COV is 5.2%. The shear failure modes and the comparison of load versus vertical displacement curves are depicted in Figs. 5 and 6, respectively. The difference between the initial slope of test and FE curves are due to the possible flexibility of the test rig in laboratory tests and this behaviour is difficult to simulate through FE models. Nonetheless, the FE model predictions shown acceptable results with the experimental behaviour.

It can be noticed that FE models well replicated the ultimate load, load-displacement relationship, and failure modes. Therefore, it can be concluded that the assumed modelling techniques provide accurate and consistent predictions of the shear response of HFCFS beams with and without concrete infill.

3. Parametric study and results

3.1. General

Since the validated models are capable of predicting the shear capacities of CF-HFCFS beams, the validated FE models were then used to evaluate the key influential paraments on the shear characteristics of HFCFS beams with lightweight normal and lightweight

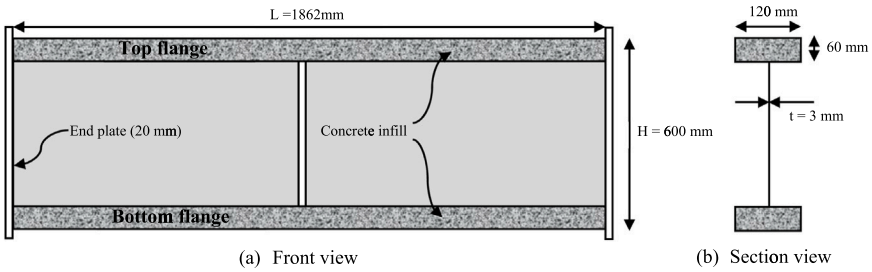

Fig. 4. The dimensions of the beam used for testing by Wang et al. [29].

Table 1
Comparison of shear capacities from tests [5] and [29] and FE models.

Researchers	Specimen (mm)	Test (kN)	FE (kN)	Test/FE
Keerthan and Mahendran [5]	150 × 45 × 2.0	68.5	69.0	0.99
	200 × 60 × 2.0	88.2	86.4	1.02
	200 × 60 × 2.5	119.3	116.5	1.02
	250 × 60 × 2.0	90.1	99.5	0.91
	250 × 75 × 2.5	139.6	139.4	1.00
	300 × 75 × 2.5	143.7	155.5	0.92
Wang et al. [29]	FWG	425.2	410.6	1.04
	Mean			0.99
	COV			5.2%

Note: Specimen notations as defined in [5] and [29].

high strength concretes. Three commonly used HFCFS sections were selected, and the section notations are given in Fig. 7. This research looked at two different lightweight concrete grades: one with a normal strength of 30 MPa and another with a strength of 50 MPa (high strength). If the strength grade of the concrete is greater than 40 MPa, it is termed high strength, according to ACI 231R-14 [47]. Additionally, two steel strengths of 350 MPa and 450 MPa were examined, as well as two steel thicknesses (2 and 3 mm). Since, Keerthan and Mahendran [48] demonstrated that corners had no effect on shear buckling capacity, corners were ignored. The aspect ratio – the ratio between the clear web height (d_1) and the clear length between two WSPs (L) was maintained as 1.0 to facilitate the failure to be purely by shear as illustrated in Fig. 8. Furthermore, the lateral displacement at the mid-points of the shear panel, as shown in Fig. 8 (Point A) was measured and plotted with the load obtained.

3.2. Analysis of the parametric study results

The results of the parametric study were given in Table 2. Apparently, the ultimate shear capacity was increased with the steel strength as well as with the section dimensions. The presence of the lightweight concrete positively impacted the shear carrying capacity of the sections. The shear capacity of all the specimens with concert infill was increased because the infilled concrete stiffens the flange and delayed the shear buckling propagation. For the specimen 150 × 90 × 15 × 3 mm with a steel grade of 350 and a concrete grade of 50 MPa, the greatest increase percentage of eight was recorded. However, it is worth noting that the concrete grade had just a little impact on the shear capacity as the load was mostly taken by the web and starts buckling before the concrete contributes to its fullest potential. The load versus the vertical displacement variation of HFCFS beams with and without concrete infill was presented in Fig. 9, which exhibits that the initial stiffnesses of both the curves were almost similar until the load reaches its maximum, and the load capacity increased for the specimen with concrete infill due to the stiffened flange.

The failure mode progression was illustrated in Fig. 10, which shows that the failure progression of the CF-HFCFS beam was guided by the linear elastic buckling mode of the beam and the load was distributed to the other parts of the beam after buckling occurred. From the failure mode, the web starts to buckle by shear when the load reached around 75% of its ultimate. During this time the diagonal strut was fully yielded, and the load was continuously distributed to the other parts of the web until the web was fully utilised. The failure modes exhibit that failure occurred purely by shear as the aspect ratio of the effective web was maintained as 1.0.

The load versus lateral displacement of two specimens (200 × 120 × 20 × 2 and 150 × 90 × 15 × 3) obtained in parametric analyses are presented in Fig. 11 for comprehension. From the illustration, the effect of thickness of the steel plate also plays a critical role in determining the shear capacity. The plate started to buckle continuously, if the thickness was low, whereas the shear buckling was delayed until the load reached closer to its maximum for the beams when the thickness is high. This was clear by the gradient of the load versus lateral displacement curves. Moreover, the post-buckling capacity was high for the specimens with concrete infill as the presence of infill delayed the shear buckling. The post-buckling capacity was relatively high for the specimens with higher thickness compared to small thickness specimens. Since, the parametric analyses have predicted the behaviour of CF- HFCFS beam under shear actions, the results obtained were then employed to develop analytical model in the next section.

4. Direct Strength Method

4.1. Introduction

Direct Strength Method (DSM) is an alternative design method that can be applied to estimate the ultimate capacities of CFS members. This emerging design method is found to be convenient, compared to the conventional effective method used for the CFS design. The linear elastic buckling capacity and yielding capacity are the two main inputs required for the DSM design. Further, this method is ideal to capture the possible post-buckling strength and inelastic reserve beyond the yielding limit. The Eurocode, i.e. EN1993-1-3 [49], includes limited design procedures for the DSM design, while other international design standards (North American, Australian, and New Zealand), AISI S100 [50] and AS/NZS 4600 [51], include a detailed procedure for DSM design. The existing DSM for CFS is extended herein to estimate the ultimate shear capacity of CF-HFCFS beams.

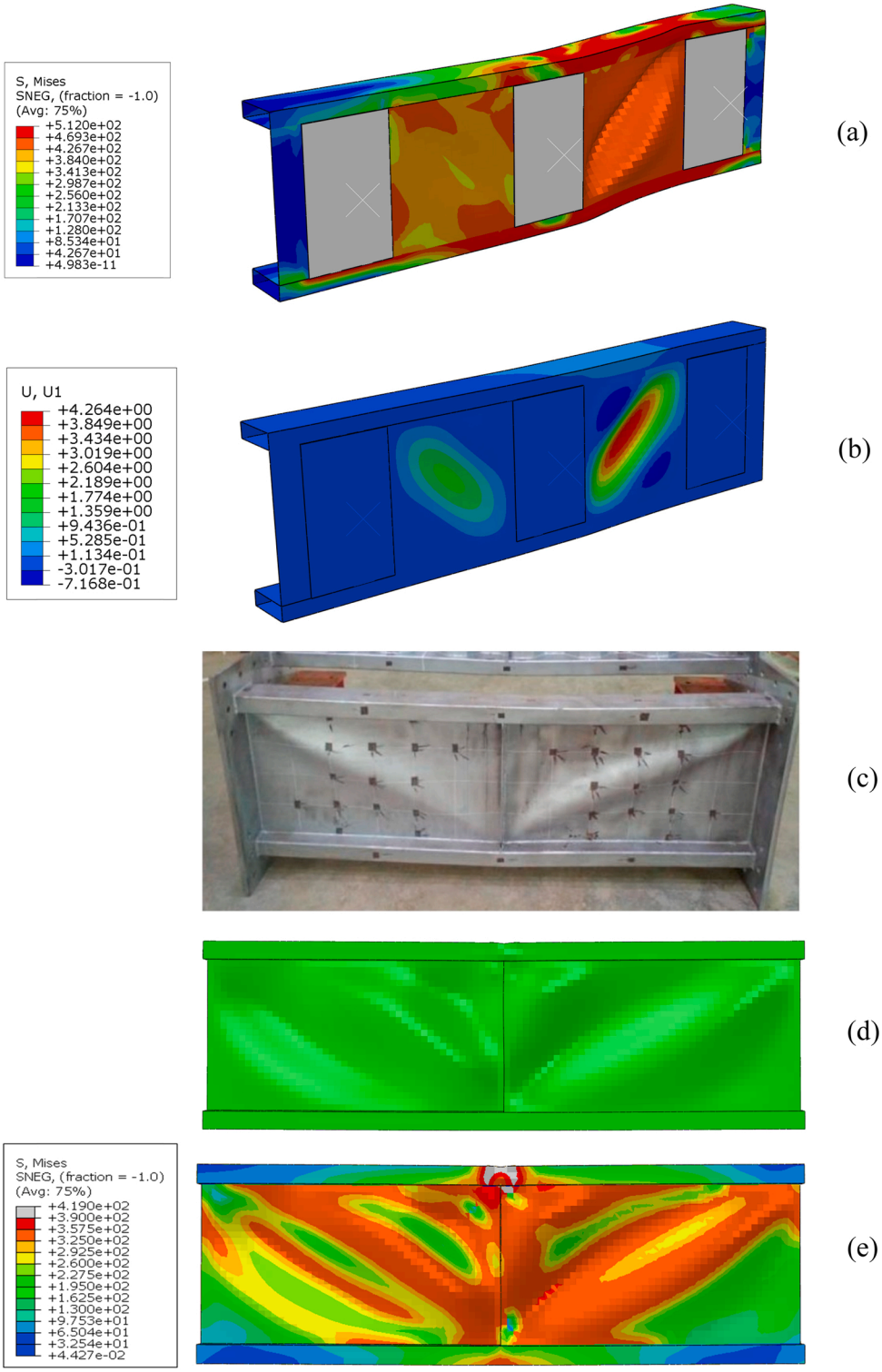

Fig. 5. Failure modes: (a, b) Specimen 150 × 45×2.0 mm (without concrete infill), (c) Specimen FWG with concrete infill (test) [29], (d) FE model of specimen FWG with concrete infill (deformed shape), (e) FE model of specimen FWG with concrete infill (deformed shape with stress contour).

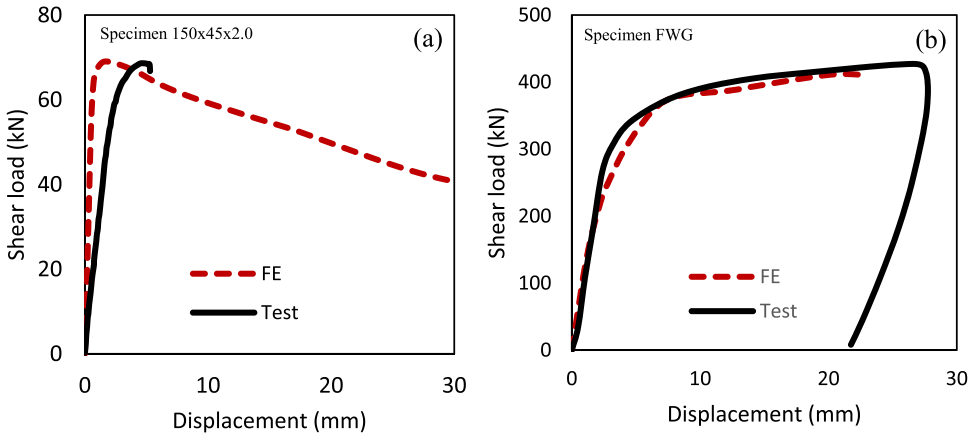

Fig. 6. Load vs vertical displacement relationship between test results((a) [5], (b) [29]) and FE model result.

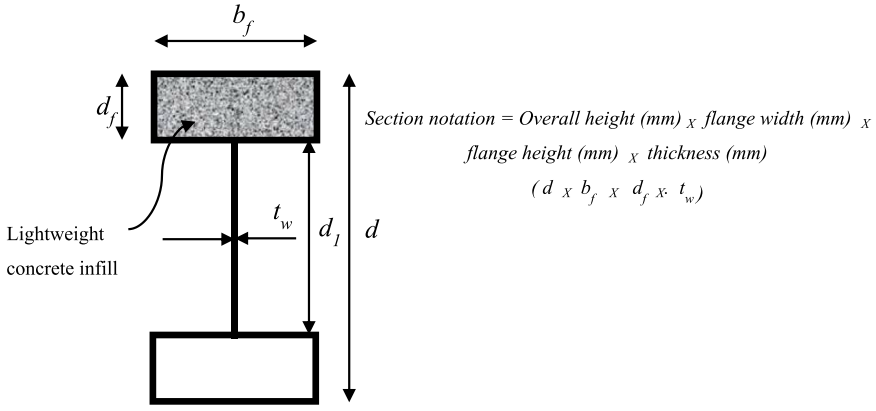

Fig. 7. Notation of the specimen for the parametric study.

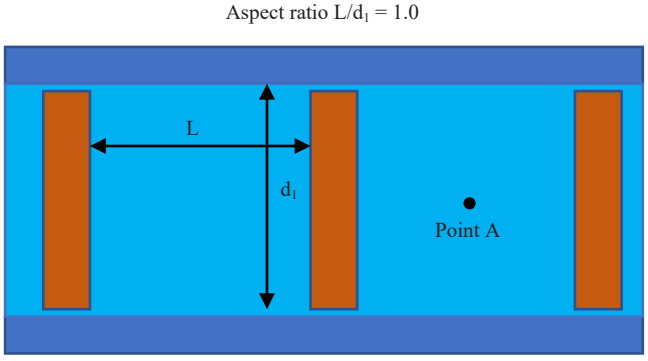

Fig. 8. . Schematic diagram of CF-HFCFS beam.

4.2. Current DSM design equations

The AISI S100 [50] and AS/NZS 4600 [51] provide identical DSM design approaches for the shear design of CFS members, where they are based on Pham and Hancock [52]. These shear design equations capture the post-buckling strength (tension field action) and the degree of web-flange fixity level which influences the ultimate shear strength. The elastic shear buckling strength, shear yielding strength and ultimate shear capacity for CFS beams with transverse web stiffeners can be determined as follow:

- Elastic shear buckling capacity (V_{cr})

Table 2
Parametric study results.

Specimen (d x b_f x d_f x t_w) (mm)	f_c (MPa)	f_y (MPa)	V_{ult} (kN)	Specimen (d x b_f x d_f x t_w) (mm)	f_c (MPa)	f_y (MPa)	V_{ult} (kN)
150 × 90 × 15 × 2	–	350	50.27	150 × 90 × 15 × 3	50	350	92.36
	–	450	62.96			450	113.40
150 × 90 × 15 × 3	–	350	85.13	200×120×20×2	30	350	63.22
	–	450	107.00			450	79.44
200×120×20×2	–	350	61.41		50	350	63.20
	–	450	76.85			450	79.57
200×120×20×3	–	350	102.43	200×120×20×3	30	350	104.40
	–	450	129.90			450	132.10
250×150×25×2	–	350	71.62		50	350	104.54
	–	450	88.64			450	132.24
250×150×25×3	–	350	120.60	250×150×25×2	30	350	74.20
	–	450	152.00			450	92.81
150 × 90 × 15 × 2	30	350	51.10		50	350	74.21
		450	64.70			450	92.96
	50	350	51.18	250×150×25×3	30	350	123.30
		450	64.72			450	155.50
150 × 90 × 15 × 3	30	350	89.88		50	350	123.44
		450	112.90			450	155.94

Note: f_c – Compressive strength of concrete, f_y – Yield strength of steel, V_{ult}- Ultimate shear capacity

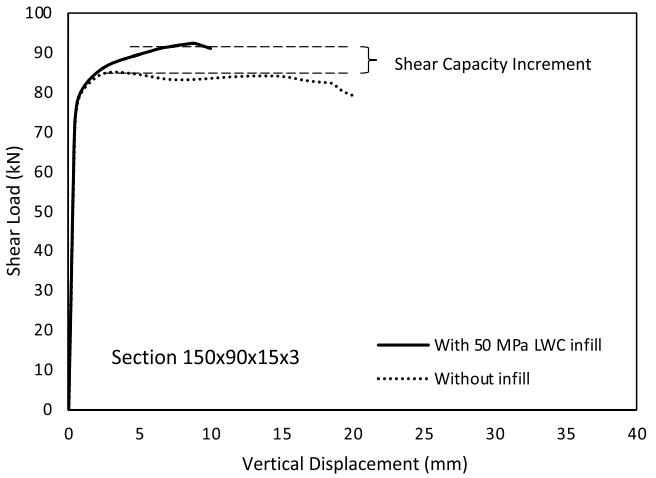

Fig. 9. Load verses vertical displacement of section 150×90×15 × 3 with and without concrete infill.

$$V_{cr} = \frac{k_v \pi^2 E t^3}{12 \quad (1-\nu^2) d_1} \tag{6}$$

Where, k_v is shear buckling coefficient, E is young's modulus of the material, t is thickness of the web, ν is Poisson's ratio, and d_1 is flat width of the web.

- Shear yielding capacity (V_y)

$$V_y = 0.6 A_w f_y \tag{7}$$

Where, A_w and f_y are area of the web ($d_1 t$) and yield strength, respectively.

- Ultimate shear capacity (V_v)

$$\text{For} \quad \lambda \leq 0.776 V_v = V_y \tag{8a}$$

$$\text{For} \quad \lambda > 0.776 V_v = \left[1 - 0.15\left(\frac{V_{cr}}{V_y}\right)^{0.4}\right]\left(\frac{V_{cr}}{V_y}\right)^{0.4} V_y \tag{8b}$$

Where, λ is the slenderness of web ($\sqrt{V_y/V_{cr}}$).

The elastic shear buckling coefficient can be calculated based on the simple equations proposed by Keerthan and Mahendran [53]. These have been included in the Appendix D3 of AS/NZS 4600 [51]. The current DSM curve and the plotted FE results are depicted in

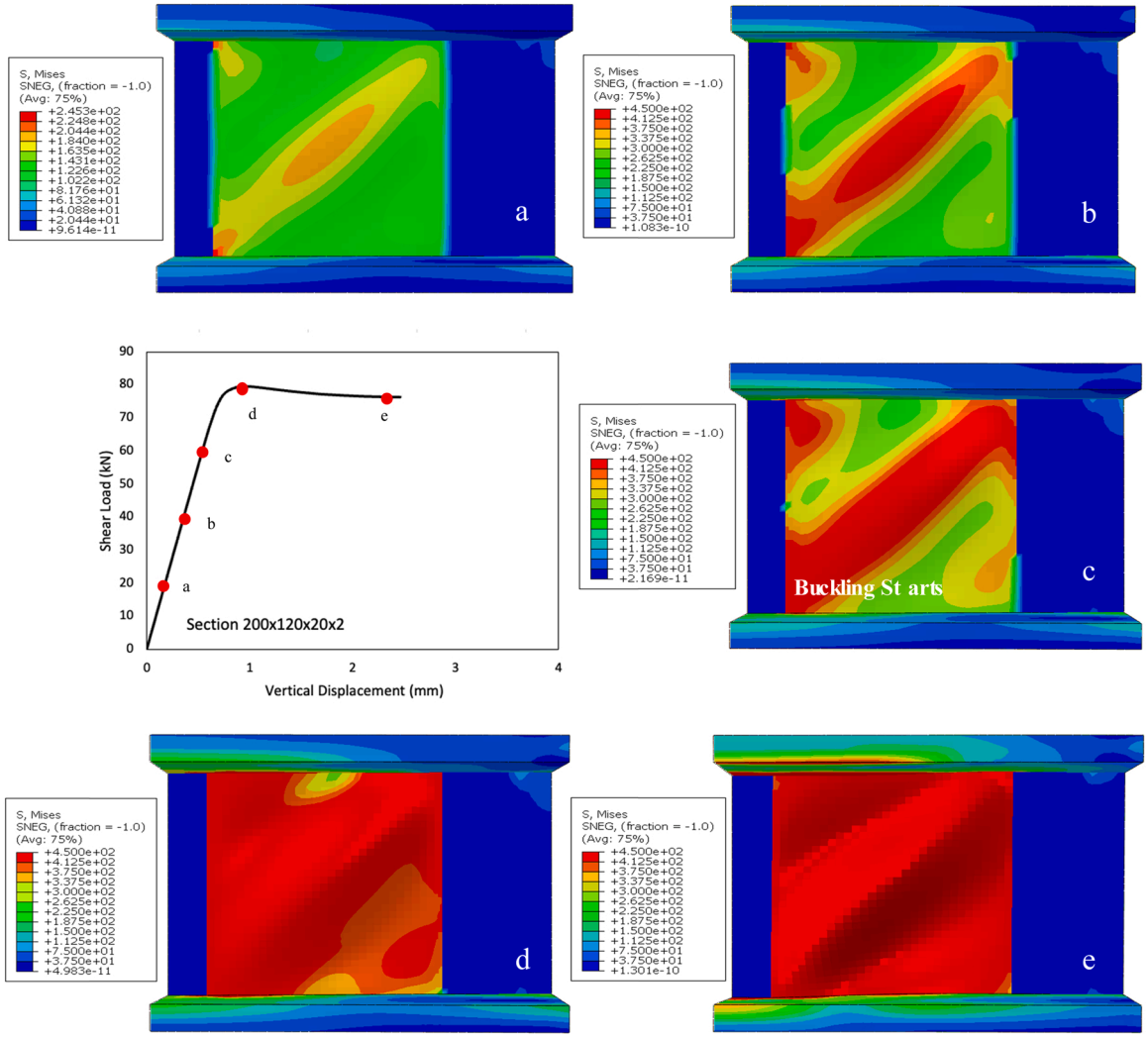

Fig. 10. Failure mode progression of section 200×120×20 × 2 with vertical displacement.

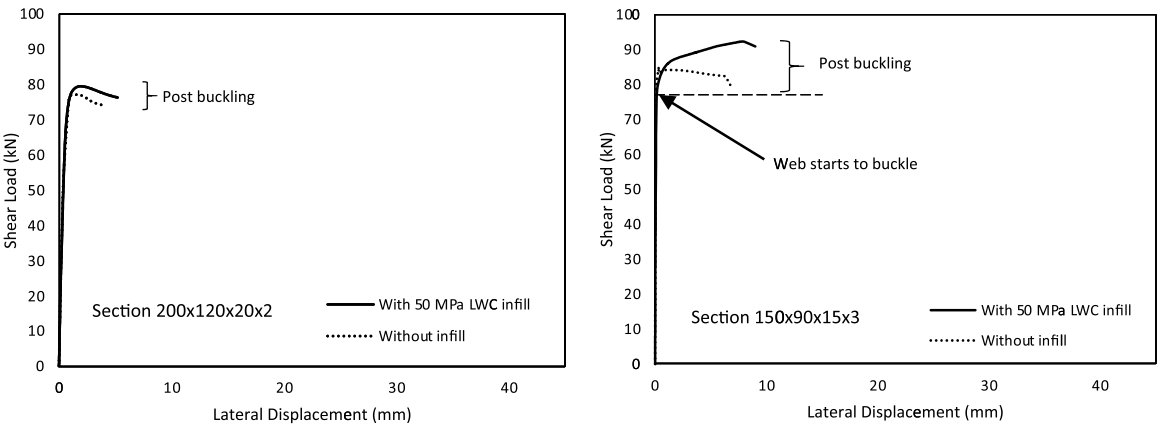

Fig. 11. Load verses lateral displacement of section 200×120×20 × 2 and 150×90×15 × 3 with and without concrete infill.

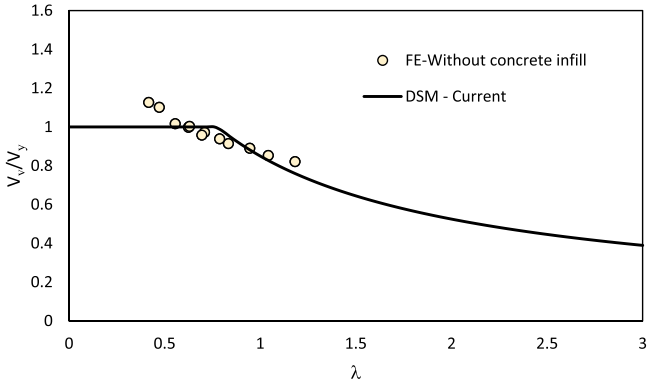

Fig. 12. Current DSM curve and FE results for hollow flange CFS channels without concrete infill.

Fig. 12.

Recently, Chandramohan et al. [54] investigated the shear behaviour of CFS channels with rectangular hollow flanges, which is similar to the sections considered in this paper. They observed inelastic reserve at the yielding region and over-conservatism of the current DSM at high slenderness. The proposed improved DSM shear design equations for CFS beams with rectangular hollow flanges are given below in Eqs. (9a and 9b).

$$\text{For} \quad 0.4 < \lambda \leq 0.703 V_v = \left[1 + 0.33\left(1 - \frac{\lambda}{0.703}\right)\right] V_y \tag{9a}$$

$$\text{For} \quad \lambda > 0.703 V_v = \left[1 - 0.13\left(\frac{V_{cr}}{V_y}\right)^{0.23}\right]\left(\frac{V_{cr}}{V_y}\right)^{0.23} V_y \tag{9b}$$

The DSM curve proposed by Chandramohan et al. [54] and the plotted FE results are shown in Fig. 13. It can be observed that the FE results without concrete infill are agreed well with Chandramohan et al. [54] DSM curve compared to the current DSM curve.

4.3. Proposed design approach

From the parametric study, it was observed that lightweight concrete infill contributes to slight improvements in ultimate shear capacities compared to the HFCFS beam without infill. The increment of the shear capacity can be captured by proposing an improvement factor that can be directly applied to the ultimate shear capacity of the CFS hollow flange beams without concrete infill. This relationship can be explained through the Eq. (10) given below.

$$V_{v,\ infill} = V_v q_s \tag{10}$$

Where, $V_{v,infill}$ is the ultimate shear capacity with lightweight concrete infill, V_v is the ultimate shear capacity without concrete infill (bare specimen), and q_s represents an improvement factor.

Fig. 14 shows the FE results of the HFCFS beams with and without concrete infill plotted against the DSM curve proposed by Chandramohan et al. [54]. It should be noted that the FE data points for the concrete infill were determined considering the ultimate capacities of the concrete infill, while the elastic shear buckling and shear yielding capacities were determined using Eqs. (6 and 7). As a result, the data points for the concrete infill specimens take higher V_v/V_y values compared to those without concrete infill (bare) specimens. The application of the improvement factor q_s to the points of concrete infilled specimens will merge the data points with concrete specimens without concrete infill and provide a simplified design method.

The improvement factor q_s was developed as a function of the compressive strength of concrete (f_c) and yield strength of the steel (f_y) as they could be responsible for the improvement in shear capacity. The relationship for q_s is formulated as given in Eq. (11):

$$q_s = 1 + \left(\frac{f_c}{f_y}\right)^a \tag{11}$$

Where, a is the coefficient to be determined from parametric study results. The accurate value for the parameter a was calculated through the class genetic algorithm in conjunction with the generalised reduced gradient solver method. The objective function was set to result in a mean value of 1.00 for the ratios between q_s values from the FE analysis and proposed q_s values while achieving a minimum COV value at the same time. From the refining process, a suitable value for a was found, shown in Eq. (12). The refining process resulted in a mean value of 1.0 and a COV value of 2% for the corresponding a value. Fig. 15 depicts the comparison of the proposed q_s against the q_s values obtained from FE analyses.

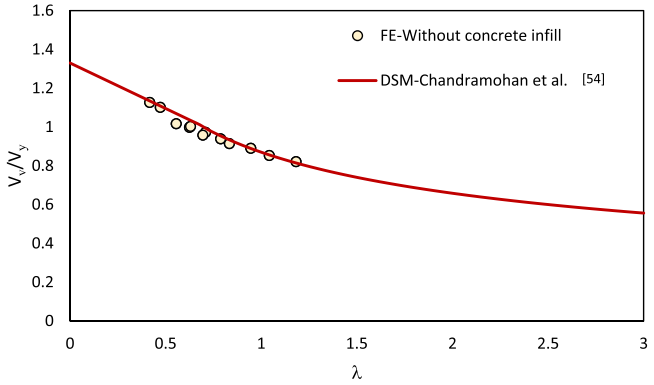

Fig. 13. DSM curve proposed by Chandramohan et al. [54] and FE results for hollow flange CFS channels without concrete infill.

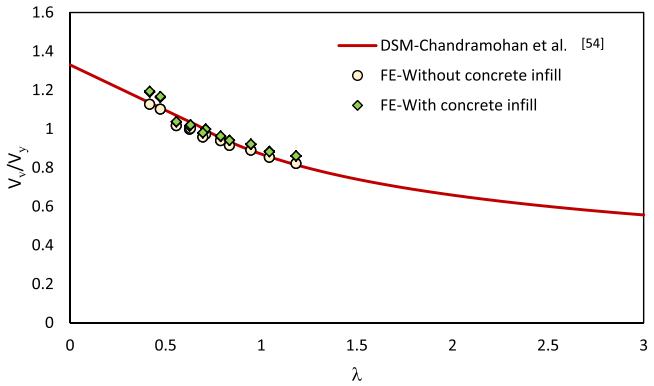

Fig. 14. DSM curve proposed by Chandramohan et al. [54] and FE results for hollow flange CFS channels without and with concrete infill.

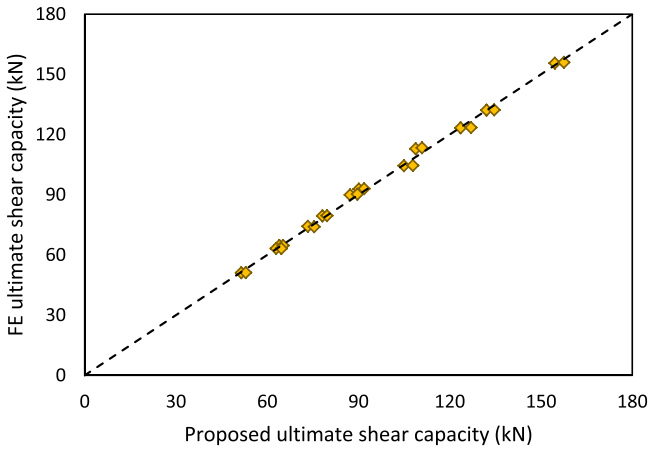

Fig. 15. Comparison of the ultimate shear capacities for concrete infilled specimens from FE and using proposed q_s equation.

$$q_s = 1 + \left(\frac{f_c}{f_y}\right)^{1.507} \tag{12}$$

For the simplified design approach for the lightweight concrete infilled HFCFS beams, the proposed q_s was incorporated into the DSM equations proposed by Chandramohan et al. [54]. Therefore, the modified DSM equations for the lightweight concrete infilled CFS hollow flange beams can be written as in Eqs. (13a and 13b). Here q_s is proposed in Eq. (12). Fig. 16 shows the FE results of the CF-HFCFS beams with the application of the proposed improvement factor q_s. It can be observed that the application of q_s merges the

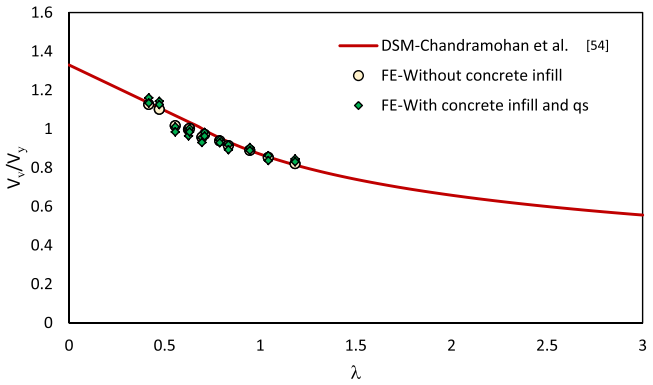

Fig. 16. DSM curve and the data points of the concrete infilled specimens from FE and using proposed q_s equation.

data points of the specimens with lightweight concrete infill with specimens without concrete infill. Therefore, the proposed simplified DSM approach can be effectively used to estimate the ultimate shear capacity of the HFCFS beams with lightweight concrete infill.

$$\text{For} \quad 0.4 < \lambda \leq 0.703 V_v = \left[1 + 0.33\left(1 - \frac{\lambda}{0.703}\right)\right] V_y. \quad q_s \tag{13a}$$

$$\text{For} \quad \lambda > 0.703 V_v = \left[1 - 0.13\left(\frac{V_{cr}}{V_y}\right)^{0.23}\right]\left(\frac{V_{cr}}{V_y}\right)^{0.23} V_y.q_s \tag{13b}$$

5. Conclusions

This study has investigated the shear performance of HFCFS beams filled with lightweight concrete based on 3D FE numerical simulations, which has been used to develop a simplified design equation to predict the ultimate shear capacities of CF-HFCFS beams. Based on the investigation, the following conclusions can be drawn.

- The developed FE numerical models can be used to predict the shear behaviour of CF-HFCFS beams as they showed a good agreement between the test results for both with and without concrete infill with overall mean and COV of 0.99 and 5.2%, respectively.
- The lightweight concrete infill had a positive impact on the ultimate shear capacity as it stiffened the flange and delayed the shear buckling, thereby increasing the ultimate shear capacity.
- The effect of concrete grade on the shear capacity improvement was minimal, however, the presence of lightweight concrete increased the post-buckling capacity to improve the shear capacity.
- A simplified design guideline was developed by using the modified DSM to predict the ultimate shear capacity of HFCFS beams filled with lightweight concrete. It can be stated from the proposed design equation with mean value of 1.00 and the COV of 2%, that it can be used to accurately predict the ultimate shear capacity of HFCFS beams with lightweight concrete infill.

In terms of limitations, the simulated FE models purposefully excluded bending and lateral torsional failure in order to mimic the models failing primarily by shear. As a result, the design equations were constructed with these limitations in mind, and the equations may change depending on the shape of the CF-HFCFS beam sections.

CRediT authorship contribution statement

Mohamed Sifan: Software, Investigation, Methodology, Formal analysis, Writing – original draft. **Perampalam Gatheeshgar**: Conceptualization, Investigation, Formal analysis, Writing – original draft. **Brabha Nagaratnam**: Supervision, Writing – review & editing. **Keerthan Poologanathan**: Conceptualization, Supervision, Project administration, Writing – review & editing. **Satheeskumar Navaratnam**: Writing – original draft. **Julian Thamboo**: Writing – review & editing. **Marco Corradi**: Writing – review & editing.

Declaration of Competing Interest

The authors declare that they have no known competing financial interests or personal relationships that could have appeared to influence the work reported in this paper.

Acknowledgements

The relevant technical, financial, and other necessary research facilities were contributed by Northumbria University.

References

[1] M. Macdonald, M. Heiyantuduwa, J. Rhodes, Recent developments in the design of cold-formed steel members and structures, Thin Walled Struct. 46 (7–9) (2008) 1047–1053.
[2] F. Gao, F. Yang, H. Liang, H. Zhu, Numerical study and strength model of concrete-filled high-strength tubular flange beam under mid-span load, Eng. Struct. 229 (2021), 111654.
[3] R. Siahaan, P. Keerthan, M. Mahendran, Lateral distortional buckling of rivet fastened rectangular hollow flange channel beams, J. Constr. Steel Res. 144 (2018) 295–309.
[4] B. Chen, K. Roy, Z. Fang, A. Uzzaman, Y. Chi, J.B. Lim, Web crippling capacity of fastened cold-formed steel channels with edge-stiffened web holes, un-stiffened web holes and plain webs under two-flange loading, Thin Walled Struct. 163 (2021), 107666.
[5] P. Keerthan, M. Mahendran, Experimental studies on the shear behaviour and strength of LiteSteel beams, Eng. Struct. 32 (10) (2010) 3235–3247.
[6] M. Hassanein, Fundamental behaviour of concrete-filled pentagonal flange plate girders under shear, Thin Walled Struct. 95 (2015) 221–230.
[7] A.-y Jiang, J. Chen, W.-l Jin, Experimental investigation and design of thin-walled concrete-filled steel tubes subject to bending, Thin Walled Struct. 63 (2013) 44–50.
[8] Y. Shao, Y. Wang, Experimental study on static behavior of I-girder with concrete-filled rectangular flange and corrugated web under concentrated load at mid-span, Eng. Struct. 130 (2017) 124–141.
[9] W. Li, H. Liang, Y. Lu, J. Xue, Z. Liu, Axial behavior of slender RC square columns strengthened with circular steel tube and sandwiched concrete jackets, Eng. Struct. 179 (2019) 423–437.
[10] F. Gao, F. Yang, H. Zhu, H. Liang, Lateral-torsional buckling behaviour of concrete-filled high-strength steel tubular flange beams under mid-span load, J. Constr. Steel Res. 176 (2021), 106398.
[11] F. Gao, H. Zhu, D. Zhang, T. Fang, Experimental investigation on flexural behavior of concrete-filled pentagonal flange beam under concentrated loading, Thin Walled Struct. 84 (2014) 214–225.
[12] M.F. Javed, N.R. Sulong, S.A. Memon, S.K.U. Rehman, N.B. Khan, FE modelling of the flexural behaviour of square and rectangular steel tubes filled with normal and high strength concrete, Thin Walled Struct. 119 (2017) 470–481.
[13] S. Li, W. Chen, Y. Zhang, Flexural behavior of precast, prestressed, lightweight aggregate concrete-conventional concrete composite beams, Constr. Build. Mater. 274 (2021), 121926.
[14] J. Zhang, Y. Huang, G. Ma, Y. Yuan, B. Nener, Automating the mixture design of lightweight foamed concrete using multi-objective firefly algorithm and support vector regression, Cem. Concr. Compos. 121 (2021), 104103.
[15] A.A. Al-Shaar, M.T. Göğüş, Flexural behavior of lightweight concrete and self-compacting concrete-filled steel tube beams, J. Constr. Steel Res. 149 (2018) 153–164.
[16] A.M. Abou-Rayan, N.N. Khalil, A.A. Zaky, Experimental investigation on the flexural behavior of steel cold-formed I-beam with strengthened hollow tubular flanges, Thin Walled Struct. 155 (2020).
[17] H. Liu, M. Elchalakani, A. Karrech, S. Yehia, B. Yang, High strength flowable lightweight concrete incorporating low C3A cement, silica fume, stalite and macro-polyfelin polymer fibres, Constr. Build. Mater. 281 (2021).
[18] F.Bd Souza, O.R.K. Montedo, R.L. Grassi, E.G.P. Antunes, Lightweight high-strength concrete with the use of waste cenosphere as fine aggregate, Matéria 24 (2019).
[19] Y. Zhou, G. Gong, Y. Huang, C. Chen, D. Huang, Z. Chen, M. Guo, Feasibility of incorporating recycled fine aggregate in high performance green lightweight engineered cementitious composites, J. Clean. Prod. 280 (2021).
[20] K.M.A. Sohel, K. Al-Jabri, M.H. Zhang, J.Y.R. Liew, Flexural fatigue behavior of ultra-lightweight cement composite and high strength lightweight aggregate concrete, Constr. Build. Mater. 173 (2018) 90–100.
[21] A. Trabelsi, Z. Kammoun, Mechanical properties and impact resistance of a high-strength lightweight concrete incorporating prickly pear fibres, Constr. Build. Mater. 262 (2020).
[22] A. Allahverdi, S.A. Azimi, M. Alibabaie, Development of multi-strength grade green lightweight reactive powder concrete using expanded polystyrene beads, Constr. Build. Mater. 172 (2018) 457–467.
[23] M.S. Nadesan, P. Dinakar, Mix design and properties of fly ash waste lightweight aggregates in structural lightweight concrete, Case Stud. Constr. Mater. 7 (2017) 336–347.
[24] Y. Wu, J.-Y. Wang, P.J.M. Monteiro, M.-H. Zhang, Development of ultra-lightweight cement composites with low thermal conductivity and high specific strength for energy efficient buildings, Constr. Build. Mater. 87 (2015) 100–112.
[25] J.-B. Yan, J.-Y. Wang, J.Y.R. Liew, X. Qian, Applications of ultra-lightweight cement composite in flat slabs and double skin composite structures, Constr. Build. Mater. 111 (2016) 774–793.
[26] Z. Huang, J.Y.R. Liew, Steel-concrete-steel sandwich composite structures subjected to extreme loads, Int. J. Steel Struct. 16 (4) (2016) 1009–1028.
[27] Z. Huang, K. Padmaja, S. Li, J.Y.R. Liew, Mechanical properties and microstructure of ultra-lightweight cement composites with fly ash cenospheres after exposure to high temperatures, Constr. Build. Mater. 164 (2018) 760–774.
[28] M. Sifan, P. Gatheeshgar, S. Navaratnam, B. Nagaratnam, K. Poologanathan, J. Thamboo, T. Suntharalingam, Flexural behaviour and design of hollow flange cold-formed steel beam filled with lightweight normal and lightweight high strength concrete, J. Build. Eng. (2021), 103878.
[29] Y. Wang, Y. Shao, C. Chen, U. Katwal, Prediction of flexural and shear yielding strength of short span I-girders with concrete-filled tubular flanges and corrugated web-I: experimental test, Thin Walled Struct. 148 (2020), 106592.
[30] Y. Wang, Y. Shao, C. Chen, U. Katwal, Prediction of flexural and shear yielding strength of short span I-girders with concrete-filled tubular flanges and corrugated web-II: Numerical simulation and theoretical analysis, Thin Walled Struct. 148 (2020), 106593.
[31] ABAQUS, Finite Element Software Documentation, Dassault Systèmes Simulia Corporation, Providence, RI, 2021.
[32] D. Dissanayake, C. Zhou, K. Poologanathan, S. Gunalan, K. Tsavdaridis, J. Guss, Numerical simulation and design of stainless steel hollow flange beams under shear, J. Constr. Steel Res. 176 (2021), 106414.
[33] M.S. Mohamed, J.A. Thamboo, T. Jeyakaran, Experimental and numerical assessment of the flexural behaviour of semi-precast-reinforced concrete slabs, Adv. Struct. Eng. 23 (9) (2020) 1865–1879.
[34] A. Espinos, L. Gardner, M.L. Romero, A. Hospitaler, Fire behaviour of concrete filled elliptical steel columns, Thin Walled Struct. 49 (2) (2011) 239–255.
[35] X. Yun, L. Gardner, The continuous strength method for the design of cold-formed steel non-slender tubular cross-sections, Eng. Struct. 175 (2018) 549–564.
[36] S. Afshan, B. Rossi, L. Gardner, Strength enhancements in cold-formed structural sections—Part I: material testing, J. Constr. Steel Res. 83 (2013) 177–188.
[37] P. Gatheeshgar, S. Parker, K. Askew, K. Poologanathan, S. Navaratnam, A. McIntosh, D.W. Small, Flexural Behaviour and Design of Modular Construction Optimised Beams, Structures, Elsevier,, 2021, pp. 1048–1068.
[38] P. Keerthan, M. Mahendran, D. Hughes, Numerical studies and design of hollow flange channel beams subject to combined bending and shear actions, Eng. Struct. 75 (2014) 197–212.
[39] A.W. Al Zand, E. Hosseinpour, W.H.W. Badaruzzaman, M.M. Ali, Z.M. Yaseen, A.N. Hanoon, Performance of the novel C-purlin tubular beams filled with recycled-lightweight concrete strengthened with CFRP sheet, J. Build. Eng. 43 (2021), 102532.

[40] J.C. Lim, T. Ozbakkaloglu, Stress–strain model for normal- and light-weight concretes under uniaxial and triaxial compression, Constr. Build. Mater. 71 (2014) 492–509.
[41] D. Lam, X. Dai, L. Han, Q. Ren, W. Li, Behaviour of inclined, tapered and STS square CFST stub columns subjected to axial load, Thin Walled Struct. 54 (2012) 94–105.
[42] L.-H. Han, G.-H. Yao, Z. Tao, Performance of concrete-filled thin-walled steel tubes under pure torsion, Thin Walled Struct. 45 (1) (2007) 24–36.
[43] P. Keerthan, M. Mahendran, New design rules for the shear strength of LiteSteel beams with web openings, J. Struct. Eng. 139 (5) (2013) 640–656.
[44] P. Keerthan, M. Mahendran, Numerical modeling of litesteel beams subject to shear, J. Struct. Eng. 137 (12) (2011) 1428–1439.
[45] Z. Tao, B. Uy, F.-Y. Liao, L.-H. Han, Nonlinear analysis of concrete-filled square stainless steel stub columns under axial compression, J. Constr. Steel Res. 67 (11) (2011) 1719–1732.
[46] P. Keerthan, Shear Behaviour and Design of LiteSteel Beams, Faculty of Environmental and Engineering, Queensland University of Technology, 2010.
[47] ACI Committee 213R-14, Guide for Structural Lightweight-aggregate Concrete, American Concrete Institute, USA, 2014.
[48] P. Keerthan, M. Mahendran, Elastic shear buckling characteristics of LiteSteel beams, J. Constr. Steel Res. 66 (11) (2010) 1309–1319.
[49] CEN, Eurocode 3 - Design of steel structures - Part 1–3 General rules- Supplementary rules for cold-formed members and sheeting, European Committee for Standardization, Brussels, 2006.
[50] AISI-S100, North American Specification for the Design of Cold-Formed Steel Structural Members, American Iron and Steel Institute, 2016.
[51] AS/NZS-4600, Australian/New Zealand Standard Cold-formed steel structures, Sydney, Australia, 2018.
[52] C.H. Pham, G.J. Hancock, Direct strength design of cold-formed C-sections for shear and combined actions, J. Struct. Eng. 138 (6) (2012) 759–768.
[53] K. Pologanathan, M. Mahendran, Improved shear design rules of cold-formed steel beams, Eng. Struct. 99 (2015) 603–615.
[54] D.L. Chandramohan, E. Kanthasamy, P. Gatheeshgar, K. Pologanathan, M.F.M. Ishqy, T. Suntharalingam, T. Kajaharan, Shear behaviour and design of doubly symmetric hollow flange beam with web openings, J. Constr. Steel Res. 185 (2021).